analytical chemistry

pubs.acs.org/ac Article

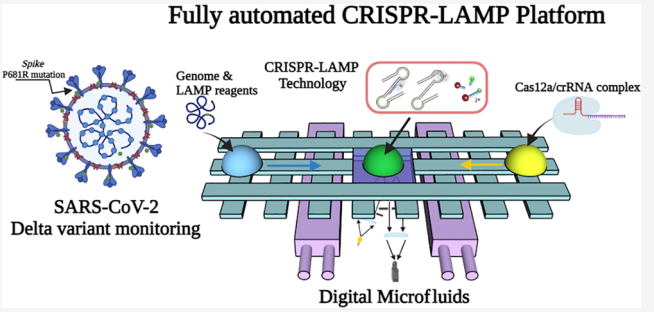
Fully Automated CRISPR-LAMP Platform for SARS-CoV-2 Delta and Omicron Variants

Tong Zhang, Wang Zhao, Xi Chen, Xinlian Zhang, Jinhui Zhu, Shenwei Li, Chuanyong Wu, Zhengan Tian,* and Guodong Sui*

Cite This: https://doi.org/10.1021/acs.analchem.2c03607 Read Online

ACCESS | Metrics & More | Article Recommendations | Supporting Information

ABSTRACT: Integrated clustered regularly interspaced short palindromic repeat (CRISPR)−loop-mediated amplification (LAMP) technology is of great importance in CRISPR-based diagnostic systems, which urgently needs to be developed to improve diagnostic accuracy. A labor-free, contamination-free, and fully automated droplet manipulation platform for the CRISPR-LAMP technology has not been developed before. Herein, we propose a fully automated CRISPR-LAMP platform, which can precisely manipulate the CRISPR-LAMP droplet and perform combined reactions with high sensitivity and specificity. SARS-CoV-2 *Spike* T478K, D614G, P681R, and P681H mutations, typical point mutations of B.1.617.2 (Delta) and Omicron variants, are monitored with this platform with a detection limit of 10^2 copies/μL. Allele discrimination between the mutants and wild type is significant with the designed one/two-mismatch CRISPR RNA (crRNA) at a limit of 10^2 copies/μL. Chemically synthesized and modified crRNAs greatly increase the CRISPR-LAMP signal, which advance the wide application. Combined with the previously developed *RdRp* CRISPR-LAMP assay, clinical results showed that *Spike* T478K and P681H can discriminate the mutant type form the wild type with 70% (49.66−85.50%, 95% confidence interval) and 78% (57.27−90.62%, 95% confidence interval) sensitivity, respectively, and 100% specificity (51.68−100%, 95% confidence interval), and the *RdRp* target can detect SARS-CoV-2 strains with 85% sensitivity (65.39−95.14%, 95% confidence interval) and 100% specificity (51.68−100%, 95% confidence interval). We believe that this automatic digital microfluid (DMF) system can advance the integrated CRISPR-LAMP technology with higher stability, sensitivity, and practicability, also for other CRISPR-associated diagnostic platforms.



Downloaded via SHANGHAI NORMAL UNIV on October 29, 2022 at 09:00:42 (UTC).
See https://pubs.acs.org/sharingguidelines for options on how to legitimately share published articles.

INTRODUCTION

Clustered regularly interspaced short palindromic repeat (CRISPR)-based diagnostic (CRISPR-Dx) systems usually combine the isothermal amplification technology with CRISPR-associated protein to precisely quantify unidentified microorganisms.[1−3] Loop-mediated amplification (LAMP) and recombinase polymerase amplification (RPA) stand out from numerous isothermal amplification methods for their robustness, sensitivity, availability, and so on.[4,5] In the meantime, CRISPR-associated protein combined with a nucleic acid amplification technology, such as CRISPR-LAMP and CRISPR-RPA, has been widely developed.[2] For a CRISPR-Dx system, a two-step reaction (target amplification followed by CRISPR-based detection) and one-step reaction (target amplification and CRISPR-based detection integrated together in one pot) are two main research branches. During the one-step reaction progress, buffer compatibility between the amplification progress and the cleavage progress restricted the CRISPR-RPA reaction efficiency. In addition, inconsistent reaction temperature between the amplification progress and cleavage progress was a limitation for the CRISPR-LAMP integrated reaction.[6] Nowadays, there are hardly any feasible solutions for one-step CRISPR-Dx reactions. During the two-step reaction progress, maximizing the CRISPR-Dx reaction rate and preventing aerosol contamination (opening tubes to manipulate the first-step reaction product) were the research emphasis.[7] Owing to the multiple amplicons of the LAMP reaction, aerosol contamination was more easily generated in open-tube operations (than PCR). Labor-reduced, contamination-free, and easily operating methods for two-step reactions need to be urgently developed. Coronavirus disease 2019 (COVID-19) exploded in 2019, in Wuhan, China, and has been widely spreading throughout the globe. Owing to its high transmission and infection rate, severe acute respiratory syndrome coronavirus-2 (SARS-CoV-2) quickly mutated,

Received: August 17, 2022
Accepted: October 12, 2022

ACS Publications © XXXX American Chemical Society

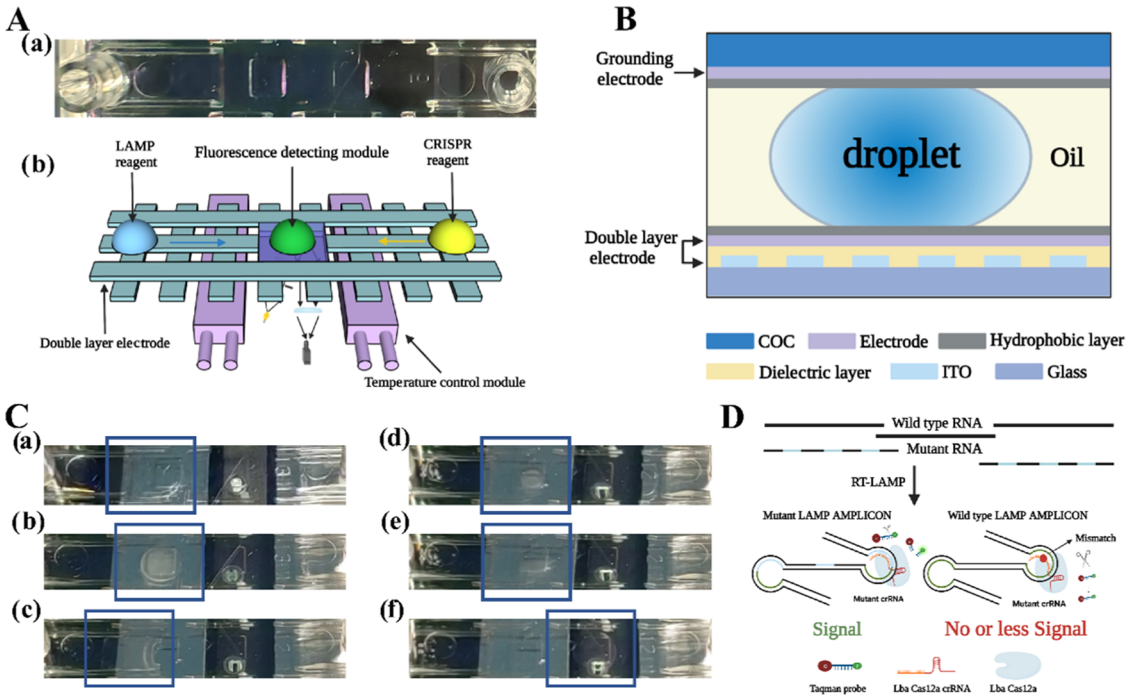


Figure 1. Design and operation of the fully automated CRISPR-LAMP platform. (A) Illustration of this DMF system. (a) Photograph of the DMF chip basic unit. (b) Schematic illustration of the automated CRISPR-LAMP system. (B) Schematic of the cross-section through the electrode array. (C) Picture clip captures of the CRISPR-LAMP reaction on the DMF chip. The blue rectangle-labeled areas show the movement of the droplet. (a) LAMP reagents move to the reaction zone. (b) LAMP reaction is finished. (c) LAMP amplicons return to the inlet and prepare to split the droplet. (d) 2−5 μL LAMP droplet is split and stays at the LAMP reaction zone. (e) CRISPR reagents merge and mix with the split LAMP droplet. (f) Final droplet moves to the fluorescence-detecting zone. (D) Mechanism of the CRISPR-LAMP technology.

especially in the *Spike* gene, which is essential for virus escape.[8] Nowadays, highly pathogenic and transmitted variants of SARS-CoV-2, Delta variant (B.1.617.2) and Omicron variant, defined as variants of concern (VOC) by the WHO, have given rise to another public health crisis.[9] Monitoring point mutations between these variants was in urgent need to characterize the virus variants, controlling another widespread explosion.

Digital microfluids (DMF) can precisely manipulate nanoliter- to microliter-sized droplets with a programmable electrode array.[10] Based on the electrowetting-on-dielectric (EWOD) phenomenon, a DMF device can control individual droplets to split, merge, and mix.[11] A series of potentials can be applied to electrodes, which will change the surface tension of the droplets, driving its movement. By arranging the electrode array, a droplet can also move in a self-designed path, which was suitable for multistep operations. Compared with other microfluidic chips, DMF chips can precisely manipulate the movement of a designated droplet with only the electrode array, and the valve design is not necessary in these chips, simplifying manufacturing operations. Researchers have successfully applied DMF chips in cycle-to-cycle amplification,[12] LAMP,[13] and RPA[14] to simplify operations. Herein, to settle the problems of the two-step CRISPR-LAMP technology, we develop fully automated digital microfluids to perform the two-step CRISPR-LAMP assay, which can prevent aerosol contamination and maximize the CRISPR-LAMP reaction rate. Dominating point mutations (*Spike* T478K, D614G, P681H, P681R) and common *RdRp* detection assay were developed based on our previously established CRISPR-LAMP technology. We can successfully detect both wild and mutant SARS-CoV-2 and simultaneously monitor the T478K, D614G, P681H, and P681R mutations in 10^2 copies/μL. To improve CRISPR efficiency, CRSIPR RNAs (crRNAs) are chemically synthesized and modified. We accidentally found that 2′-*O*-methyl 3′phosphorothioate modification can significantly reduce the fluorescence background. Combining these improvements, we utilize clinical samples with wild, Delta, and Omicron strains to verify the CRISPR-LAMP system. Results show that *RdRp* CRISPR-LAMP assay can detect almost all the three virus strains (85% sensitivity, 65.39−95.14%, 95% confidence interval). P681H (78% sensitivity, 57.27−90.62%, 95% confidence interval) and D614G (85% sensitivity, 65.39−95.14%, 95% confidence interval) CRISPR-LAMP assay can discriminate the above-mentioned three virus strains, and T478K CRISPR-LAMP assay can be an alternative (70% sensitivity). To the best of our knowledge, this is the first time to combine DMF with the CRISPR-LAMP technology. This programmable system has great potential in precise pathogen diagnosis and can be integrated into fully automated diagnostic platforms.

EXPERIMENTAL SECTION

DMF Chip Fabrication. The structure of the sandwiched DMF chip is shown in Figure 1B. It consisted of double-layer indium tin oxide (ITO)-coated bottom glass patterned with a laser to form the vertical drive electrodes and a top copolymer of cycloolefin (COC) with the grounding electrode. A 10 μm SU-8 photoresist was spin-coated and developed between the double vertical electrodes as the dielectric layer following the procedure given by Microchem. Then, both the bottom and top plates were coated with 200 nm Teflon AF1600 as the hydrophobic layer facilitating the movement of the droplet. The two plates were separated with a 200 μm conductive tape,

https://doi.org/10.1021/acs.analchem.2c03607
Anal. Chem. XXXX, XXX, XXX−XXX

and the space was filled with silicon oil (1 cSt), used as the reaction room. The silicon oil could not only prevent aerosol pollution but also prevent nonspecific adsorption of organics in reaction reagents.

DMF System Assembly. The real chip reaction unit and system structure illustration are shown in Figure 1A. The instrument consisted of a droplet control system, custom software, a fluorescence detector, and temperature control modules. The designed DMF cartridge placed above the fluorescence detector was temperature-controlled using two temperature control modules. The chip was connected to the driving system via 48-pin interfaces and controlled using software, which can charge the electrodes in a certain sequence. Sinusoidal wave signals (100 Vrms, 10 kHz) were generated to drive the droplets between the top plate (ground electrode) and the bottom plate.

DMF System and Droplet Manipulation. LAMP reagents and CRISPR reagents are first added into both sides of the chip inlet, and then, temperature control modules and driving electrodes are controlled in sequence (Figure 1C). (1) One temperature module is heated to 63 °C, and the other semiconductor is kept at 25 °C. (2) LAMP reagents are moved to the heating zone (Figure 1C-a) and kept at 63 °C for 45 min (Figure 1C-b). (3) The temperature of the LAMP reaction zone is lowered to 37 °C, and the other is increased to 37 °C. (4) LAMP amplicons (white precipitates) are moved to the chip inlet (Figure 1C-c), and a 2−5 μL droplet is separated and moved back to the LAMP reaction zone (Figure 1C-d). (5) CRISPR reagents are moved from the other inlet to the LAMP reaction zone, merging and mixing with LAMP amplicons (Figure 1C-e). (6) The mixing droplet is moved to the fluorescence-detecting zone (between the two temperature zones) (Figure 1C-f). (7) Fluorescence is collected once per minute for 15−30 min and processed using the DMF system. The full time of the whole procedure is 45−75 min.

Point Mutation Detection Design. For *Spike* T478K, D614G, and P681R/H common LAMP primer design, point mutation sites (C22995A, A23403G, C23604G/A) should be put in F2−F1, F1−B1c, or B2c−B1c sites (or the corresponding complementary sequence) and screened carefully with their free energy (http://primerexplorer.jp/e/index.html). Then, sensitivity assays were performed to screen suitable primer pairs. The crRNA sequence should be put in the primer no-binding position, especially the seed sequence with the mismatch design position. One-mismatch and two-mismatch crRNAs were designed,[2] and a 20−24 nt spacer sequence was adjusted according to the calculated RNA structure (http://www.unafold.org/mfold/applications/rna-folding-form.php).[15] The LAMP primer sequence disturbs, and spacer sequence cross-interference with other pathogens was also calculated with NCBI BLAST web tools (https://blast.ncbi.nlm.nih.gov/Blast.cgi). All the primer sequence, plasmid sequence, and spacer sequence are shown in Tables S2 and S3. *RdRp* LAMP primers and crRNAs were verified and shown in our previous study.[16]

crRNA Synthesis. For the biological crRNA synthesis progress, the forward Lbacas12a sequence (/5/AATTCTAATACGACTCACTATAGGTAATTTCTACTAAGTGTAGAT/3/) and reverse Lbacas12a sequence (/5/ spacer sequence complementary + ATCTACACTTA-GTAGAAATTACC/3/) were PCR-amplified and purified. Then, the purified fragments were transcribed with a Hiscribe T7 high-yield RNA synthesis kit for 16 h at 37 °C and afterward purified with a Monarch RNA cleanup kit. The transcribed crRNAs were quantified with Qubit FLEX RNA HS assay and stored at −80 °C for later use. For the chemical crRNA synthesis progress, the whole crRNA sequence was synthesized using bioligo (Shanghai, China). 2′-*O*-Methyl 3′phosphorothioate was incorporated at three terminal nucleotides at the 5′ end and two terminal nucleotides at the 3′ end.

Other materials and methods are shown in the Supporting Information.

RESULTS AND DISCUSSION

Fully Automated CRISPR-LAMP (FACL) Platform. We first developed a DMF chip for the CRISPR-LAMP technology, and this is illustrated in Figure 1. The basic DMF unit was composed of two inlets, two temperature control sections, and a fluorescence detection section (Figure 1A). The droplet embedded between the top substrate and bottom substrate was controlled by bottom double vertical electrode arrays, and silicone oil was filled in to prevent aerosol contamination (Figure 1B). LAMP assay was performed in the chip with visible white pyrophosphoric acid precipitates and then split into two parts, in which the small part (2−5 μL) of the double-stranded LAMP amplicons was then merged with the preloaded CRISPR reagents to perform cleavage assay (Figure 1C,D). Detailed illustration of the CRISPR-LAMP DMF chip is shown in Supporting Videos S1−S3, separately introducing the LAMP reaction, LAMP product splitting, and merging between separated LAMP amplicons and CRISPR reagents. With the DMF chip, CRISPR-LAMP assay can be divided into two steps automatically and combined operations can be precisely manipulated with no risk of aerosol contamination. Previously, we described in detail in-tube two-step CRISPR-LAMP assay by introducing a uracil-DNA glycosylase (UDG) system.[16] This system could efficiently clear the incorporated 2′-deoxyuridine 5′-triphosphate (dUTP) in the previous CRISPR-LAMP system, preventing aerosol contamination for UDG can remove the dUTP-incorporated amplicons. However, an extra incorporated dUTP in the CRISPR-LAMP system may decrease reaction sensitivity within limited time. In addition, extra labor was necessary for this combined technology. For two-step CRISPR-Dx platforms, we summarized different methods (CRISPR-LAMP, CRISPR-RPA, and CRISPR-PCR), and these are shown in Table S1. Like UDG and Cas9/sgRNA pretreatment measures,[7,17] they could decrease aerosol contamination in amplification. While performing the second cleavage assay, open-tube measures might introduce another cross-contamination. For separated chip operations, almost all reaction reagents were put into the final cleavage assay, which might decrease the sensitivity of CRISPR-Dx platforms for the buffer compatibility.[18,19] For common microfluid chips, precise droplet manipulation usually needs valve design or complex external instruments, which might increase the complexity of these diagnostic systems. Our proposed fully automated CRISPR-LAMP platform (FACL) utilized digital microfluid technology to precisely manipulate droplets, in which typically, 2 μL of LAMP amplicons, split from 25 μL of LAMP final products, was merged and mixed with 18 μL of CRISPR reagents. These programmable splitting, merging, and mixing operations could decrease the influence of the LAMP reaction buffer on CRISPR cleavage assay, and aerosol contamination was prevented from the silicone oil in the DMF chip. These basic DMF units (Figure 1A-a) could be copied simultaneously

https://doi.org/10.1021/acs.analchem.2c03607
Anal. Chem. XXXX, XXX, XXX−XXX

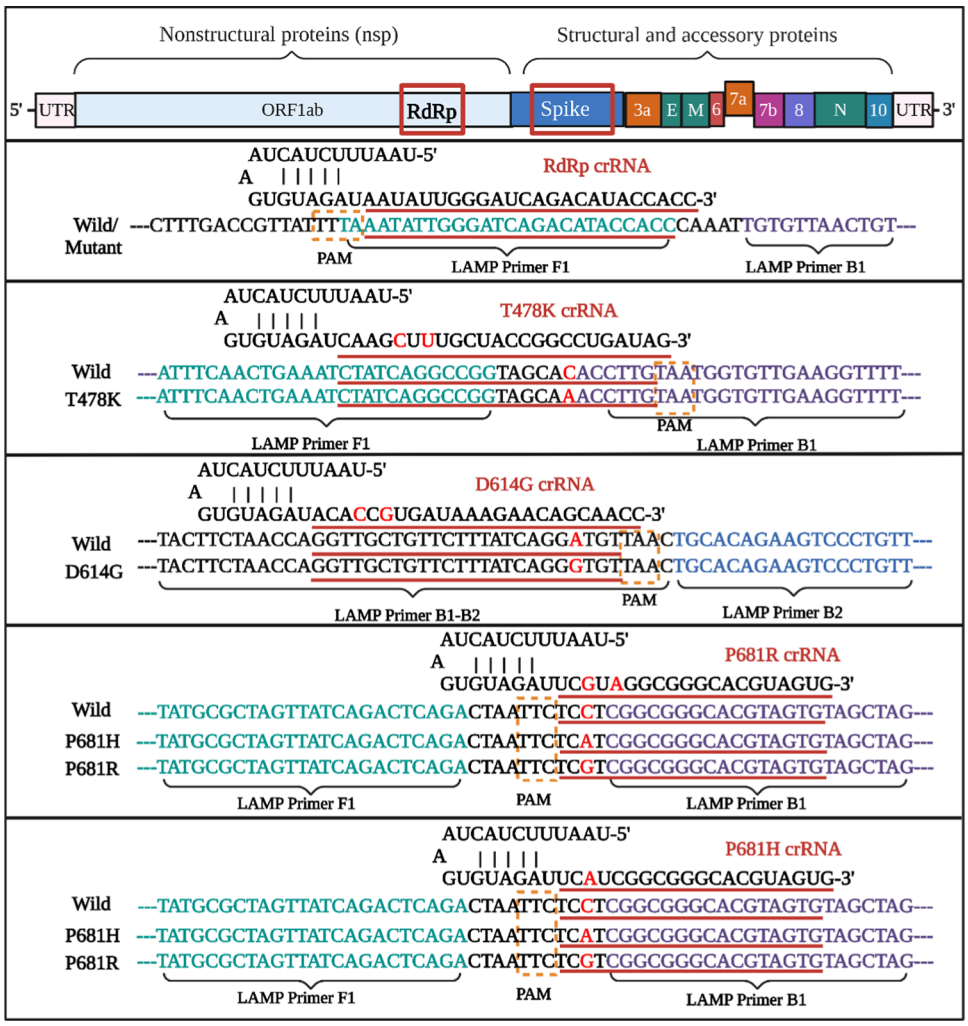


Figure 2. Design of CRISPR-LAMP technology-based diagnosis of SARS-CoV-2 variants. SARS-CoV-2 genome map and designed site of crRNA in *RdRp* and *Spike* gene. PAM = protospacer adjacent motif. Red line under nucleotide sequence were paired nucleotide between target and crRNA. Red base in target and crRNA were mutant points.

in a single chip, which could improve the diagnostic throughput. Nowadays, we could simultaneously perform 16 CRISPR-LAMP assays in a single chip within 1 h.

Common and Specific CRISPR-LAMP Designs. Owing to the high infectivity and transmissibility of SARS-CoV-2 Delta and Omicron variants, point mutations of concern should be monitored to protect public health. Comparing the B.1617.2 (Delta variant) sequence and Omicron variant among the Nextstrain clade, GISAID clade, and Pango lineage, we found that *Spike* T478K, D614G, P681R, and P681H were special point mutations for the widespread characteristics all over these clades. Also, studies have shown that mutations at the *Spike* residue positions 478, 614, and 681 (located at a furin cleavage site) may result in higher pathogenicity and transmissibility.[20−22] Summarized from Nextstrain CoVariants resources, residue positions 478 and 681 existed only in Delta and Omicron strains and residue position 614 existed in almost all VOCs. To discriminate dominating VOCs (Delta and Omicron variants) from other VOCs, the CRISPR-LAMP technology was used to discriminate these point mutations (Figure 1D). In addition, our previously developed *RdRp* CRISPR-LAMP assay was combined with the FACL assay to ensure the existence of the SARS-CoV-2 virus, of which the LAMP primer and crRNA sequence are very conserved among VOCs.[16] The CRISPR-LAMP design illustration is shown in Figure 2. The PAM sequence of *Lachnospiraceae bacterium ND2006* (Lba) Cas12a can be TTTV or TTV. The crRNA sequence of the common CRISPR-LAMP technology (like the *RdRp* target) can be located anywhere in the LAMP primer position F3-B3 without affecting cleavage efficiency. For specific CRISPR-LAMP technology, point mutations should be included in LAMP amplicons with no binding of primers. The spacer sequence of specific crRNA can have one mismatch and two mismatch to improve allele discrimination. For the one-mismatch (P681H crRNA) pair, the third position of the spacer sequence was chosen to discriminate P681H (C23604A point mutation). For the two-mismatch (T478K crRNA, D614G crRNA, and P681R crRNA) pair, the seventh, fourth, and third positions of the spacer sequence were the initial point mutations existing in the mutant strains for T478K, D614G, and P681R, respectively, and additionally incorporated mutations in the fifth, sixth, and fifth positions of the above-mentioned three mutant types could improve allele discrimination. Sometimes, the initial position of the mismatch could not be adjusted due to its PAM sequence restriction, and the position and base type of the second incorporated mismatch could be adjusted freely to improve point mutation discrimination.

https://doi.org/10.1021/acs.analchem.2c03607
Anal. Chem. XXXX, XXX, XXX−XXX

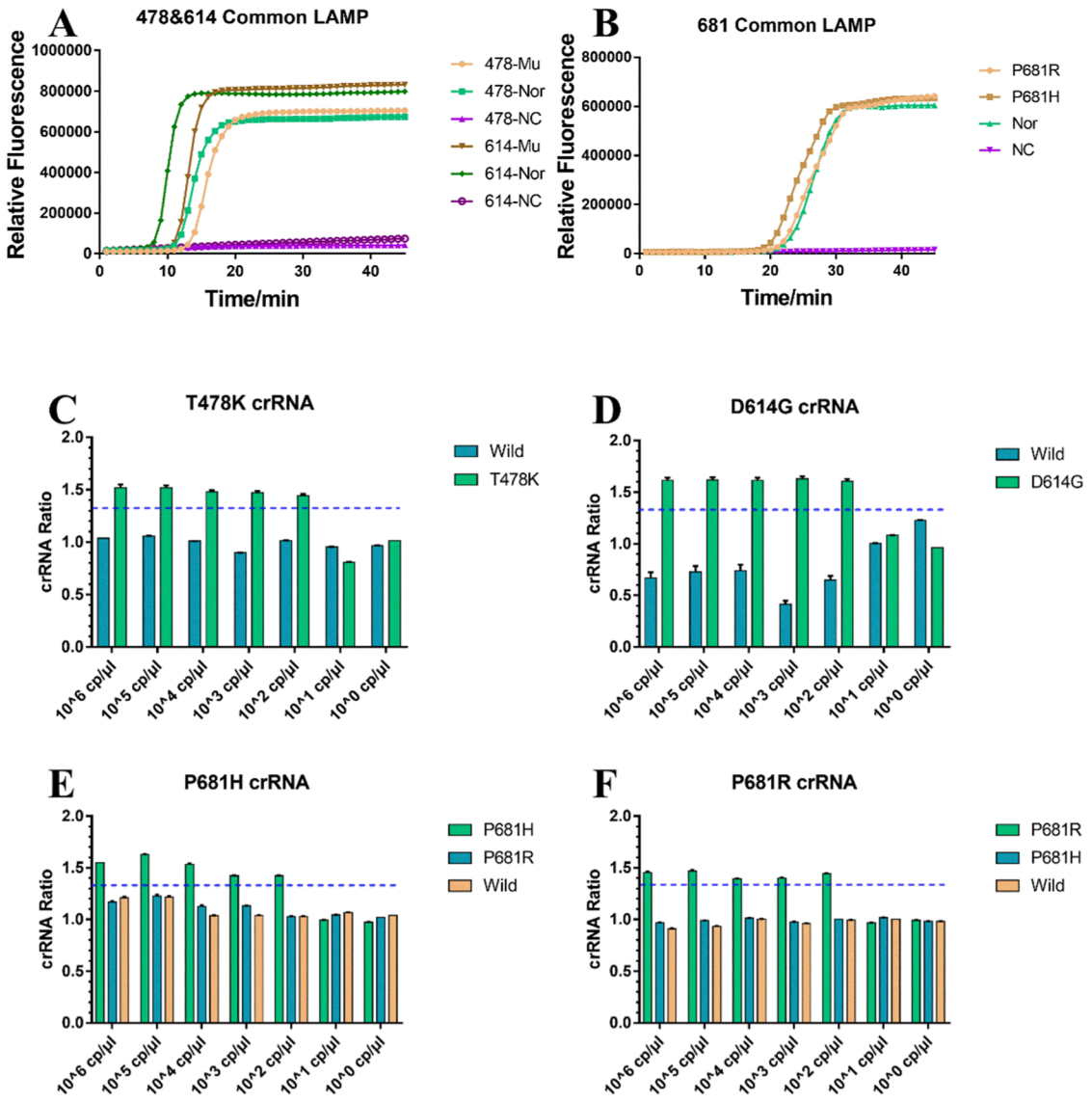


Figure 3. CRISPR-LAMP technology-based diagnosis of SARS-CoV-2. (A) Common LAMP primer screen of *Spike* 478 and 614 mutations. (B) Common LAMP primer screen of *Spike* 478 and 614 mutations. (C−F) Common CRISPR-LAMP detection efficiency with different crRNAs. The dashed line (value = 1.33) indicates the threshold of SARS-CoV-2 positive results (the fluorescence of the target is twice the background fluorescence). (n = 4 technical replicates; the bars represent mean ± SD); NC: negative control; Nor/Wild: normal SARS-CoV-2; and Mu: mutant type.

Establishment of VOC CRISPR-LAMP Assay. To detect both Delta and Omicron variants and discriminate them from other VOCs, we established specific *Spike* T478K, D614G, P681R, and P681H CRISPR-LAMP assays and common *RdRp* CRISPR-LAMP assay (established previously). First, the best common primer pairs for *Spike* 478, 614, and 681 different positions have been chosen among 1000 primer pairs, which can amplify both the wild-type and mutant SARS-CoV-2 (Figure 3A,B). Although there was an amplification bias between the wild type and mutant type for the limit of detection (LoD) for the wild and mutant types varied between 10^2 and 10^3 copies/μL (Figure S1), this minor discrimination cannot significantly discriminate the mutant and wild type (Figure S1). One-mismatch and two-mismatch crRNAs were utilized to calculate point mutation discrimination, and results showed that one-mismatch P681H crRNA and two-mismatch T478K crRNA, D614G crRNA, and P681R crRNA could efficiently discriminate point mutations from the wild type (Figure S2). The sensitivity of these crRNAs showed that these CRISPR-LAMP assays could efficiently discriminate the mutant type from the wild type, approaching 10^2 copies/μL (Figure 3C−F). For P681R and P681H crRNAs, they could also discriminate P681H and P681R mutant types, which could be utilized in the precise diagnosis of Delta and Omicron variants separately. The value of the dash line in Figure 3C−F was 1.33, which means that the fluorescence of the target was twice the background fluorescence.[23] Utilizing this standard, point mutations could be clearly discriminated from the wild type. This crRNA discrimination, utilizing the CRISPR-LAMP technology, could significantly improve the point mutation diagnostic capacity compared with the common LAMP technology (Figure 3A,B). Specificity assay of these CRISPR-LAMP assays (Figure S3) showed that T478K, D614G, P681H, and P681R had no cross-interference with other respiratory tract pathogens. The background fluorescence of the wild-type SARS-CoV-2 virus could be discriminated with

https://doi.org/10.1021/acs.analchem.2c03607
Anal. Chem. XXXX, XXX, XXX−XXX

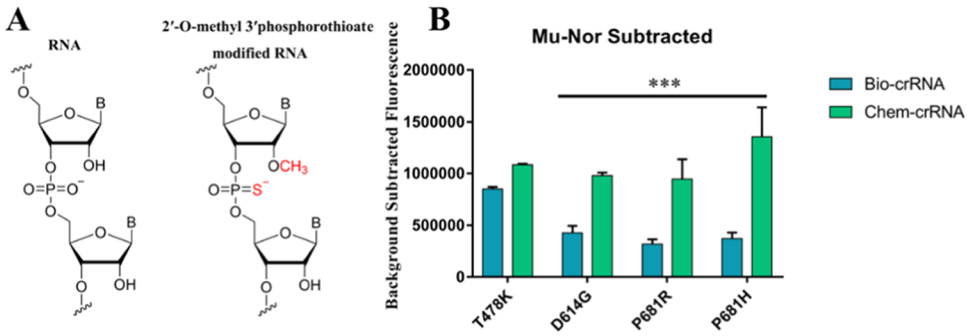


Figure 4. Influence of chemically synthesized crRNAs in the CRISPR-LAMP technology. (A) Normal RNA and 2′-*O*-methyl 3′phosphorothioate-modified RNA. (B) Fluorescence intensity between biologically and chemically synthesized crRNAs. (n = 4 technical replicates; the bars represent mean ± SD); Bio: biologically synthesized and Chem: chemically synthesized.

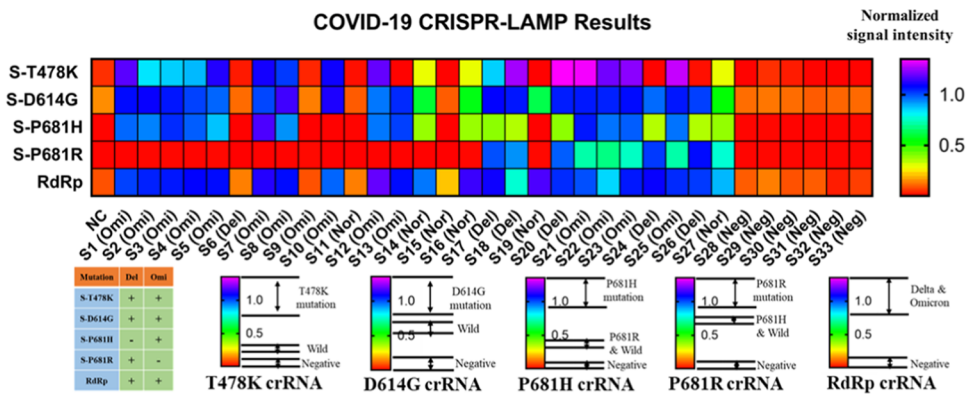


Figure 5. Clinical results of the proposed CRISPR-LAMP assay. Points mutations in Del (Delta) and Omi (Omicron) are summarized according to the Nextstrain CoVariants (https://covariants.org/); NC: negative control; Nor: normal SARS-CoV-2 samples; and Neg: negative SARS-CoV-2 samples.

the crRNA ratio equation (supplemented in the Supporting Information). Confirming common LAMP primers and specific CRISPR crRNAs is essential in the CRISPR-LAMP technology for the amplification efficiency and cleavage efficiency will significantly influence signal readouts. The fully automated CRISPR-LAMP (FACL) platform could separate LAMP and CRISPR assays with less biointerference, which greatly enlarges LAMP primer and crRNA sequence design capacity, improving the final detection signal.

Chemically Synthesized and Modified crRNAs. Conventional crRNAs are synthesized biologically with PCR amplification and transcription. The purity of biologically synthesized crRNAs cannot approach 90%, and there is always residual one−two G base before the 5′ ends (after transcription). We doubted if crRNA structure optimization and sequence integrity will influence CRISPR-LAMP fluorescence results. Researchers found that sgRNA modification with 2′-*O*-methyl and 3′phosphorothioate will improve Cas9 in vivo genome editing efficiency.[24] We doubted whether this modification and crRNA purity improvements will improve CRISPR-LAMP efficiency. Compared with biologically synthesized crRNAs, the fluorescence of the chemically synthesized crRNAs was almost twice to thrice (Figure 4B), significantly increasing the fluorescence signal. The purity of the chemically synthesized crRNAs can approach 90−95%, and chemical 2′-*O*-methyl 3′phosphorothioate modifications (Figure 4A) can stabilize the crRNA structure to prevent degradation, which may contribute mainly to the fluorescence increasing. Comparison of real-time CRISPR-LAMP fluorescence between biologically and chemically synthesized crRNAs (Figure S4) showed that there was almost no background fluorescence in the chemically synthesized crRNAs except for the D614G crRNA. However, comparison of the crRNA ratio between the biologically and chemically synthesized crRNAs showed that chemically synthesized crRNAs cannot discriminate between wild and mutant types with the dash line standard (Figure S5). We found that the lower fluorescence background in the chemically synthesized crRNAs resulted in this phenomenon. We also found that the fluorescence of wild and mutant templates spread regularly and normalized fluorescence (normalized with the positive control) can efficiently distinguish wild and mutant templates (verified in clinical trials). Differences between biologically and chemically synthesized crRNAs reminded us that unidentified crRNA sequences and structures with biological synthesis methods will sometimes ignore the real signals of point mutations and decrease signal dramatically.

Clinical Results. Utilizing chemically synthesized crRNAs in clinical trials, we collected the CRISPR-LAMP fluorescence of 33 nasopharyngeal swab specimens from Shanghai Customs Port Clinic. Normalized with the positive control, a heat map was organized for *Spike* T478K, D614G, P681H, and P681R and *RdRp* (Figure 5). The judgment standards of Delta and Omicron (according to the Nextstrain CoVariants resources) variants are shown in the left bottom of Figure 5. Real-time CRISPR-LAMP fluorescence showed that positive clinical samples spread regularly (Figure S6). Normalized with the positive control of *Spike* T478K, D614G, P681H, and P681R

https://doi.org/10.1021/acs.analchem.2c03607
Anal. Chem. XXXX, XXX, XXX−XXX

and the *RdRp* target, standards for these five targets are shown in the right bottom of Figure 5. The normalized fluorescence of the wild-type SARS-CoV-2 strain was almost 0.6 in P681R and D614G, while it was about 0.3 in T478K and P681H, which interfered less in the point mutation judgment. The normalized fluorescence of the mutant-type SARS-CoV-2 strain was almost above 0.9 in the five gene targets, showing great detection efficiency. Statistical data of these CRISPR-LAMP results showed that *Spike* T478K, D614G, and P681H, and *RdRp* have higher sensitivity (70−85% sensitivity) (Table S4, 95% confidence interval). Analyzing separately with the wild type, Delta, and Omicron strains, we found that T478K, D614G, and P681H and *RdRp* CRISPR-LAMP assays have the highest sensitivity in Omicron samples (87−93% sensitivity) and lowest sensitivity in wild-type samples (Tables S5−S7, 95% confidence interval). We thought that a common LAMP amplification bias may result in differences in the limit of detection. Additionally, we also found that samples 6, 9, 11, and 15 were undetected among all five gene targets, which meant that these samples might have very little viral loads or the quality might be influenced. Although P681R CRISPR-LAMP can distinguish almost all Delta samples, its limit of detection did not meet the clinical requirements. Considering D614G distributed in almost all VOCs, the detection priority is higher for T478K (distributed in Delta and Omicron variants) and P681H (distributed in the Omicron variant). Combining *RdRp* and *Spike* T478K and P681H CRISPR-LAMP assays, we could efficiently discriminate the wild-type, Delta, and Omicron samples. The specificity of these CRIPSR-LAMP assay was 100% (51.68−100%, 95% confidence interval) and sensitivity was 82−91% (excluding abnormal samples 6, 9, 11, 15). With improvements in the CRISPR-LAMP reaction system (like the enzyme efficiency of BST and Cas12a, reaction volume, and crRNA sequence optimization), the limit of detection may be improved to approach higher sensitivity.

Outlook. Our proposed fully automated CRISPR-LAMP (FACL) platform can precisely control the LAMP assay and CRISPR cleavage assay and maximize final fluorescence intensity without aerosol contamination. Buffer compatibility problems were clearly figured out for double vertical electrode arrays, which can precisely manipulate droplet splitting, merging, and mixing, eliminating the influence of the LAMP reaction buffer in Cas12a cleavage assay. This DMF chip can also combine the CRISPR-RPA technology for its programmable droplet manipulation. Although RPA and CRISPR cleavage assays almost have the same reaction temperature, the buffer compatibility also influences the final fluorescence intensity. In addition, multiplex reactions can be easily performed in the proposed FACL platform, for LAMP products can be precisely split into multiple parts (by double vertical electrode arrays), which can then perform CRISPR cleavage assay, not reducing detection sensitivity. Currently, another research interest is to discover new CRISPR-associated protein (that tolerates high temperature) to directly incorporate into the LAMP reaction, like *Alicyclobacillus acidiphilus* (AapCas12b),[25] *Alicyclobacillus acidoterrestris* Cas12b (AacCas12b),[26] and engineered AsCas12a.[27] However, these one-step assays are very strict with the reaction temperature, which limits the sensitivity of LAMP itself. Also, the reaction rates for the LAMP assay are slower than those of Cas/crRNA and may finally decrease the fluorescence intensity for incomplete amplification. Studies also demonstrate that the pyrophosphate precipitation in the LAMP reaction may inhibit the CRISPR cleavage assay.[27] From our point of view, the two-step CRISPR-LAMP technology may have greater potential in point-of-care testing for its higher sensitivity. Combined with a fully automated digital microfluid platform, the two-step CRISPR-LAMP technology can be advanced with more stability with no aerosol contamination, more rapid response to pathogen diagnosis with an automatic operation platform, and more practicability with multiplex reactions in a single DMF chip.

CONCLUSIONS

Herein, we proposed a FACL platform, which can precisely manipulate CRISPR-LAMP assay with high sensitivity and specificity. CRSIPR-LAMP assay of SARS-CoV-2 *Spike* T478K, D614G, P681H, and P681R mutations was also developed with a detection limit of 10^2 copies/μL. Allele discrimination was significant with the designed one-mismatch or two-mismatch crRNAs at a limit of 10^2 copies/μL. Chemically synthesized and modified crRNAs can replace biologically synthesized crRNAs to greatly increase the CRISPR-LAMP signal. Clinical sample results showed that *Spike* T478K, D614G, P681H, and *RdRp* (developed in the previous work) have 70−85% sensitivity and 100% specificity. *Spike* T478K and P681H CRISR-LAMP assays can be combined to discriminate Delta and Omicron variants from wild-type samples, and *RdRp* CRISPR-LAMP assay can be utilized to determine SARS-CoV-2 samples. This automatic DMF system can also be adapted to other CRISPR-Dx diagnostics to further advance their stability, sensitivity, and practicability, which has not been reported before. Combined with other automatic operation platforms, this DMF system can be applied widely in clinical diagnostic systems. Additionally, this DMF system can also integrate fast nucleic acid extraction and enrichment prior to the CRISPR-Dx diagnostic step in one DMF chip, which can greatly simplify the pathogen diagnostic workflow. Another extraction buffer compatibility with the DMF chip, especially the voltage and dielectric layer, should be tested. This DMF system has great potential in multiplex diagnosis, which can greatly reduce operation labor. We believe that with the aid of this DMF chip, the two-step CRISPR-LAMP technology has better sensitivity, specificity, and stability (also for other CRISPR-Dx diagnostic technologies).

ASSOCIATED CONTENT

Supporting Information

The Supporting Information is available free of charge at https://pubs.acs.org/doi/10.1021/acs.analchem.2c03607.

CRISPR-LAMP assay_LAMP droplet movement (MP4)

CRISPR-LAMP assay_LAMP droplet split (MP4)

CRISPR-LAMP assay_CRISPR-LAMP droplet merge and mix (MP4)

Materials, CRISPR-LAMP reagents, CRISPR-LAMP fluorescence data analysis, optimization of point mutation detection assay, clinical sample results, original primers, crRNA sequence, and statistical data of clinical samples (PDF)

https://doi.org/10.1021/acs.analchem.2c03607
Anal. Chem. XXXX, XXX, XXX−XXX

AUTHOR INFORMATION

Corresponding Authors

Zhengan Tian − *Shanghai International Travel Healthcare Center (Shanghai Customs Port Clinic), Shanghai 200433, P. R. China*; Email: tianzhenganciq@163.com

Guodong Sui − *Shanghai Key Laboratory of Atmospheric Particle Pollution and Prevention (LAP3), Department of Environmental Science and Engineering, Fudan University, Shanghai 200433, P. R. China; Shanghai Institute of Infectious Disease and Biosecurity, Fudan University, Shanghai 200032, P. R. China; Jiangsu Collaborative Innovation Center of Atmospheric Environment and Equipment Technology (CICAEET), Nanjing University of Information Science & Technology, Nanjing 210044, P. R. China;* orcid.org/0000-0002-6751-0852; Email: gsui@fudan.edu.cn

Authors

Tong Zhang − *Shanghai Key Laboratory of Atmospheric Particle Pollution and Prevention (LAP3), Department of Environmental Science and Engineering, Fudan University, Shanghai 200433, P. R. China*

Wang Zhao − *Shanghai Key Laboratory of Atmospheric Particle Pollution and Prevention (LAP3), Department of Environmental Science and Engineering, Fudan University, Shanghai 200433, P. R. China*

Xi Chen − *Shanghai Key Laboratory of Atmospheric Particle Pollution and Prevention (LAP3), Department of Environmental Science and Engineering, Fudan University, Shanghai 200433, P. R. China*

Xinlian Zhang − *Shanghai Key Laboratory of Atmospheric Particle Pollution and Prevention (LAP3), Department of Environmental Science and Engineering, Fudan University, Shanghai 200433, P. R. China*

Jinhui Zhu − *Shanghai Key Laboratory of Atmospheric Particle Pollution and Prevention (LAP3), Department of Environmental Science and Engineering, Fudan University, Shanghai 200433, P. R. China*

Shenwei Li − *Shanghai International Travel Healthcare Center (Shanghai Customs Port Clinic), Shanghai 200433, P. R. China*

Chuanyong Wu − *Shanghai Hengxin BioTechnology, Shanghai 200438, P. R. China*

Complete contact information is available at: https://pubs.acs.org/10.1021/acs.analchem.2c03607

Author Contributions

T.Z.: conceptualization, methodology, data curation, validation, and writing the original draft. W.Z.: conceptualization. X.C.: data curation and validation. X.Z.: investigation, film shooting, and editing. J.Z.: data curation and validation. S.L.: resources and investigation. C.W.: DMF chip resource. Z.T.: clinical sample resource and funding acquisition. G.S.: conceptualization, funding acquisition, and writing—review and editing.

Notes

The authors declare no competing financial interest.

ACKNOWLEDGMENTS

This work was supported by the COVID-19 research project for universities (Ministry of Education), Shanghai Municipal Science and Technology Major Project (ZD2021CY001), and General Administration of Customs, P. R. China (2019HK125). Figures 1 and 2 were created with BioRender.com. The DMF system was fabricated by Shanghai Hengxin BioTechnology (China).

REFERENCES

(1) Broughton, J. P.; Deng, X.; Yu, G.; Fasching, C. L.; Servellita, V.; Singh, J.; Miao, X.; Streithorst, J. A.; Granados, A.; Sotomayor-Gonzalez, A.; Zorn, K.; Gopez, A.; Hsu, E.; Gu, W.; Miller, S.; Pan, C.-Y.; Guevara, H.; Wadford, D. A.; Chen, J. S.; Chiu, C. Y. *Nat. Biotechnol.* **2020**, *38*, 870−874.

(2) Gootenberg, J. S.; Abudayyeh, O. O.; Lee, J. W.; Essletzbichler, P.; Dy, A. J.; Joung, J.; Verdine, V.; Donghia, N.; Daringer, N. M.; Freije, C. A.; Myhrvold, C.; Bhattacharyya, R. P.; Livny, J.; Regev, A.; Koonin, E. V.; Hung, D. T.; Sabeti, P. C.; Collins, J. J.; Zhang, F. *Science* **2017**, *356*, 438−442.

(3) Chen, J. S.; Ma, E.; Harrington, L. B.; Da Costa, M.; Tian, X.; Palefsky, J. M.; Doudna, J. A. *Science* **2018**, *360*, 436−439.

(4) Li, J.; Macdonald, J.; von Stetten, F. *Analyst* **2019**, *144*, 31−67.

(5) Moehling, T. J.; Choi, G.; Dugan, L. C.; Salit, M.; Meagher, R. J. *Expert Rev. Mol. Diagn.* **2021**, *21*, 43−61.

(6) Wang, B.; Wang, R.; Wang, D.; Wu, J.; Li, J.; Wang, J.; Liu, H.; Wang, Y. *Anal. Chem.* **2019**, *91*, 12156−12161.

(7) Bao, Y.; Jiang, Y.; Xiong, E.; Tian, T.; Zhang, Z.; Lv, J.; Li, Y.; Zhou, X. *ACS Sens.* **2020**, *5*, 1082−1091.

(8) Weisblum, Y.; Schmidt, F.; Zhang, F.; DaSilva, J.; Poston, D.; Lorenzi, J. C.; Muecksch, F.; Rutkowska, M.; Hoffmann, H.-H.; Michailidis, E.; Gaebler, C.; Agudelo, M.; Cho, A.; Wang, Z.; Gazumyan, A.; Cipolla, M.; Luchsinger, L.; Hillyer, C. D.; Caskey, M.; Robbiani, D. F.; Rice, C. M.; Nussenzweig, M. C.; Hatziioannou, T.; Bieniasz, P. D. *eLife* **2020**, *9*, No. e61312.

(9) Wang, Y.; Chen, R.; Hu, F.; Lan, Y.; Yang, Z.; Zhan, C.; Shi, J.; Deng, X.; Jiang, M.; Zhong, S.; Liao, B.; Deng, K.; Tang, J.; Guo, L.; Jiang, M.; Fan, Q.; Li, M.; Liu, J.; Shi, Y.; Deng, X.; Xiao, X.; Kang, M.; Li, Y.; Guan, W.; Li, Y.; Li, S.; Li, F.; Zhong, N.; Tang, X. *EClinicalMedicine* **2021**, *40*, No. 101129.

(10) Zou, F.; Ruan, Q.; Lin, X.; Zhang, M.; Song, Y.; Zhou, L.; Zhu, Z.; Lin, S.; Wang, W.; Yang, C. J. *Biosens. Bioelectron.* **2019**, *126*, 551−557.

(11) Choi, K.; Ng, A. H. C.; Fobel, R.; Wheeler, A. R. *Annu. Rev. Anal. Chem.* **2012**, *5*, 413−440.

(12) Kühnemund, M.; Witters, D.; Nilsson, M.; Lammertyn, J. *Lab Chip* **2014**, *14*, 2983−2992.

(13) Sukthang, K.; Kampeera, J.; Sriprachuabwong, C.; Kiatpathomchai, W.; Pengwang, E.; Tuantranont, A.; Wechsatol, W. *Sensors* **2021**, *21*, 3126.

(14) Kalsi, S.; Valiadi, M.; Tsaloglou, M.-N.; Parry-Jones, L.; Jacobs, A.; Watson, R.; Turner, C.; Amos, R.; Hadwen, B.; Buse, J.; Brown, C.; Sutton, M.; Morgan, H. *Lab Chip* **2015**, *15*, 3065−3075.

(15) Zuker, M. *Nucleic Acids Res.* **2003**, *31*, 3406−3415.

(16) Zhang, T.; Zhao, W.; Zhao, W.; Si, Y.; Chen, N.; Chen, X.; Zhang, X.; Fan, L.; Sui, G. *Anal. Chem.* **2021**, *93*, 16184−16193.

(17) Qian, C.; Wang, R.; Wu, H.; Zhang, F.; Wu, J.; Wang, L. *Anal. Chem.* **2019**, *91*, 11362−11366.

(18) Wu, H.; He, J.-S.; Zhang, F.; Ping, J.; Wu, J. *Anal. Chim. Acta* **2020**, *1096*, 130−137.

(19) Wu, H.; Qian, C.; Wu, C.; Wang, Z.; Wang, D.; Ye, Z.; Ping, J.; Wu, J.; Ji, F. *Biosens. Bioelectron.* **2020**, *157*, No. 112153.

(20) Rajah, M. M.; Hubert, M.; Bishop, E.; Saunders, N.; Robinot, R.; Grzelak, L.; Planas, D.; Dufloo, J.; Gellenoncourt, S.; Bongers, A.; Zivaljic, M.; Planchais, C.; Guivel-Benhassine, F.; Porrot, F.; Mouquet, H.; Chakrabarti, L.; Buchrieser, J.; Schwartz, O. *EMBO J.* **2021**, *40*, No. e108944.

(21) Cherian, S.; Potdar, V.; Jadhav, S.; Yadav, P.; Gupta, N.; Das, M.; Rakshit, P.; Singh, S.; Abraham, P.; Panda, S.; NIC team. *bioRxiv* **2021**, DOI: 10.1101/2021.04.22.440932.

(22) Saito, A.; Irie, T.; Suzuki, R.; Maemura, T.; Nasser, H.; Uriu, K.; Kosugi, Y.; Shirakawa, K.; Sadamasu, K.; Kimura, I.; Ito, J.; Wu, J.;

Iwatsuki-Horimoto, K.; Ito, M.; Yamayoshi, S.; Ozono, S.; Butlertanaka, E. P.; Tanaka, Y. L.; Shimizu, R.; Shimizu, K.; Yoshimatsu, K.; Kawabata, R.; Sakaguchi, T.; Tokunaga, K.; Yoshida, I.; Asakura, H.; Nagashima, M.; Kazuma, Y.; Nomura, R.; Horisawa, Y.; Yoshimura, K.; Takaori-Kondo, A.; Imai, M.; The Genotype to Phenotype Japan, C.; Nakagawa, S.; Ikeda, T.; Fukuhara, T.; Kawaoka, Y.; Sato, K. *bioRxiv* **2021**, DOI: 10.1101/2021.06.17.448820.

(23) Huang, Z.; Tian, D.; Liu, Y.; Lin, Z.; Lyon, C. J.; Lai, W.; Fusco, D.; Drouin, A.; Yin, X.; Hu, T.; Ning, B. *Biosens. Bioelectron.* **2020**, *164*, No. 112316.

(24) Hendel, A.; Bak, R. O.; Clark, J. T.; Kennedy, A. B.; Ryan, D. E.; Roy, S.; Steinfeld, I.; Lunstad, B. D.; Kaiser, R. J.; Wilkens, A. B.; Bacchetta, R.; Tsalenko, A.; Dellinger, D.; Bruhn, L.; Porteus, M. H. *Nat. Biotechnol.* **2015**, *33*, 985−989.

(25) Joung, J.; Ladha, A.; Saito, M.; Kim, N.-G.; Woolley, A. E.; Segel, M.; Barretto, R. P. J.; Ranu, A.; Macrae, R. K.; Faure, G.; Ioannidi, E. I.; Krajeski, R. N.; Bruneau, R.; Huang, M.-L. W.; Yu, X. G.; Li, J. Z.; Walker, B. D.; Hung, D. T.; Greninger, A. L.; Jerome, K. R.; Gootenberg, J. S.; Abudayyeh, O. O.; Zhang, F. *N. Engl. J. Med.* **2020**, *383*, 1492−1494.

(26) Li, L.; Li, S.; Wu, N.; Wu, J.; Wang, G.; Zhao, G.; Wang, J. *ACS Synth. Biol.* **2019**, *8*, 2228−2237.

(27) Ooi, K. H.; Liu, M. M.; Tay, J. W. D.; Teo, S. Y.; Kaewsapsak, P.; Jin, S.; Lee, C. K.; Hou, J.; Maurer-Stroh, S.; Lin, W.; Yan, B.; Yan, G.; Gao, Y.-G.; Tan, M. H. *Nat. Commun.* **2021**, *12*, No. 1739.

Recommended by ACS

Amplification-Free, Single-Microbead-Based Cas12a Assay for One-Step DNA Detection at the Single-Molecule Level

Xueping Yang, Jiehua Ma, *et al.*

SEPTEMBER 15, 2022
ANALYTICAL CHEMISTRY

READ

Dual-CRISPR/Cas12a-Assisted RT-RAA for Ultrasensitive SARS-CoV-2 Detection on Automated Centrifugal Microfluidics

Yong Chen, Xingyu Jiang, *et al.*

JULY 01, 2022
ANALYTICAL CHEMISTRY

READ

Sensitive Detection of a Single-Nucleotide Polymorphism in Foodborne Pathogens Using CRISPR/Cas12a-Signaling ARMS-PCR

Hao Yang, Yi Dong, *et al.*

JUNE 29, 2022
JOURNAL OF AGRICULTURAL AND FOOD CHEMISTRY

READ

One Versatile Cas9-Integrated Single-Tube Duplex Quantitative Real-Time PCR System for Rapid Analysis of CRISPR/Cas-Induced Mutants

Xueqi Li, Litao Yang, *et al.*

JULY 22, 2022
ANALYTICAL CHEMISTRY

READ

Get More Suggestions >

https://doi.org/10.1021/acs.analchem.2c03607
Anal. Chem. XXXX, XXX, XXX−XXX